Preprints of the 19th World Congress
The International Federation of Automatic Control
Cape Town, South Africa. August 24-29, 2014

Complementary Control of the Depth of an Underwater Robot

Alessandro Malerba and **Giovanni Indiveri**

Dipartimento Ingegneria Innovazione, Universita del Salento,
ISME node, via Monteroni, 73100 Lecce - Italy
(e-mail: giovanni.indiveri@unisalento.it).

Abstract: The depth control of an Autonomous Underwater Vehicle (AUV) is addressed. The vehicle is equipped with two separate actuation systems for the heave axis: a ballast tank system and a set of four jet motors generating vertical forces in the bow and stern of the vehicle. These two actuation systems have different time constants: the ballast tank system is rather slow, while the jet actuators have a much faster dynamics. The proposed control systems is inspired by the theory of complementary filtering in estimation where the output of slow sensors (low pass filters) is combined with the output of faster sensors (or the very plant model, i.e. high pass filters) to generate an estimate. In the given setting a heave controller is designed generating a desired force command. This signal is partitioned in a lower and higher frequency component: the former is sent to the ballast tank system and the latter to the jet thruster actuators. As a result, the depth force command is seemingly executed concurrently by the two actuation systems each working in its most natural frequency domain. The control design methodology is outlined and simulation results are reported illustrating the overall performance.

Keywords: Marine systems, Output regulation, Motion control, Robot control, Autonomous Vehicles

1. INTRODUCTION

Automatic depth control is one of the most basic, yet fundamental, functionalities of underwater vehicles. The task of heave control is particularly important for autonomous underwater robots that are been employed in an increasing number of application and scenarios. Since the early work [Cristi et al., 1990] many different control design methods and technologies have been applied to the problem: basic PID-based solution are described, by example, in [Zanoli and Conte, 2003], [Caccia et al., 2003] and [Alvarez et al., 2008] while a gain - scheduling approach is addressed in [Silvestre and Pascoal, 2007]. The modeling of heave dynamics of underwater vehicles together with possible control solutions is also covered in [Fossen, 1994].

Contrary to most underwater vehicles considered in the literature, this work addresses the problem of depth control for a vehicle equipped with two separate actuation systems for the heave axis: a ballast tank system and a set of four jet motors generating vertical forces in the bow and stern of the vehicle. The vehicle at hand is the Autonomous Underwater Vehicle (AUV) Folaga described in [Caffaz et al., 2010]. The two actuation systems for the heave axis have different time constants: the ballast tank system is rather slow, while the jet actuators have a much faster dynamics. The vehicle's factory - designed control system exploits either the ballast tank system or the vertical thrusters for heave command according to the mission specification. Pure vertical dive maneuvers (i.e. a zero surge) are typically controlled by the ballast tank system only while during in via point navigation depth is regulated using the vertical thrusters. The proposed solution aims at designing a control system able to concurrently exploit both actuator systems using them in their natural frequency domain. In particular, the designed controller is inspired by the theory of complementary filtering in estimation where the output of slow sensors (low pass filters) is combined with the output of faster sensors (or the very plant model, i.e. high pass filters) to generate an estimate. In the given setting a depth controller is designed generating a desired force command. This signal is partitioned in a lower and higher frequency component: the former is sent to the ballast tank system and the latter to the jet thruster actuators. As a result, the depth force command is seemingly executed concurrently by the two actuation systems.

Section 2 gives a brief overview of the complementary filtering technique and its extension to actuation as adopted in the paper. The AUV depth model used for control design is illustrated in section 3 while the resulting control solution is presented in section 4. Conclusion are finally addressed in section 5.

2. COMPLEMENTARY ACTUATION

2.1 Complementary Filtering

In general, complementary filters provide a means to fuse multiple independent noisy measurement of the same signal that have complementary spectral characteristics. Consider a signal $x(t)$ in the time domain and the related measurements $y_k(t)$ for $k = 1, 2, \ldots, N$ coming from different sensors. Assuming the sensor models to be linear, in the Laplace domain the following would hold (refer to Fig. 1):

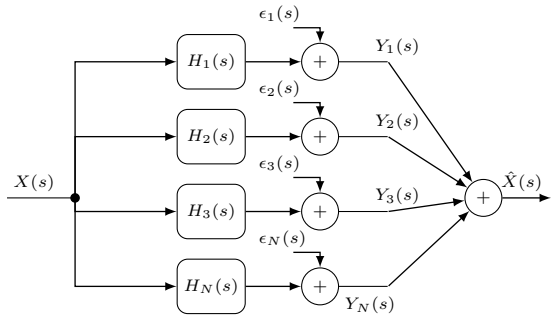

Fig. 1. Basic complementary filter for estimation.

$$Y_k(s) = H_k(s)X(s) + \epsilon_k(s) \tag{1}$$

where $H_k(s)$ is the transfer function of the k-th sensor and $\epsilon_k(s)$ is the corresponding measurement noise. Consider N proper transfer functions $P_k(s)$ for $k = 1, \ldots, N$ such that

$$\sum_{k=1}^{N} P_k(s)Y_k(s) = \left(\sum_{k=1}^{N} P_k(s)H_k(s\right) X(s) + \sum_{k=1}^{N} P_k(s)\epsilon_k(s). \tag{2}$$

If the weights $P_k(s)$ are chosen such that

$$\sum_{k=1}^{N} P_k(s)H_k(s) = 1 \quad \Longrightarrow \tag{3}$$

$$\sum_{k=1}^{N} P_k(s)Y_k(s) = X(s) + \sum_{k=1}^{N} P_k(s)\epsilon_k(s) \tag{4}$$

and assuming $P_k(s)$ and $\epsilon_k(s)$ to have orthogonal spectra for all k, i.e. $P_k(s)\epsilon_k(s) = 0 \;\forall\, k = 1, \ldots, N$ or, at least, that

$$P_k(s)\epsilon_k(s) \approx 0, \quad \forall\, k = 1, \ldots, N \tag{5}$$

the unknown signal $X(s)$ could be estimated according to

$$\hat{X}(s) = \sum_{k=1}^{N} P_k(s)Y_k(s). \tag{6}$$

Notice that the complementary estimator in equation (6) builds on the fundamental *complementary condition* $\sum_{k=1}^{N} P_k(s)H_k(s) = 1$ in equation (3).

2.2 Complementary Actuation

Assuming to have a process where an output can be controlled through more actuators, the idea of *complementary actuation* is to distribute the control effort over the actuators according to their spectral properties. Namely, the very principle of complementary filtering is exploited on the dual case of actuation. In particular, consider m actuators for the same degree of freedom. Fig.2 refers to the case $m = 2$ that corresponds to the situation at hand. In this Fig. 2 the term $R_C(s)$ is a controller for the system $G(s)$, $P_h(s)$ are weights used to distribute the control effort on the various actuators, and finally, the terms $C_h(s)$ model the actuators.

Given the plant model

$$Y(s) = G(s)U_C(s) \tag{7}$$

its input $U_C(s)$, following the set up depicted in Fig. 2, can be written as follows:

$$U_C(s) = \sum_{h=1}^{m} U_h(s) \tag{8}$$

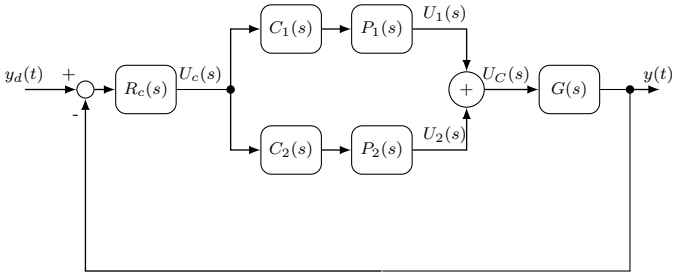

Fig. 2. A simple Complementary actuation diagram for only two actuators.

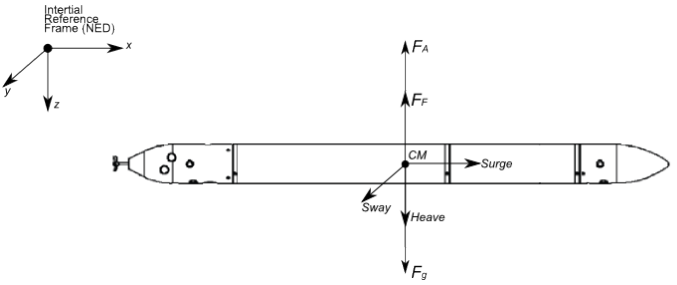

Fig. 3. Heave force balance: CM is the center of mass, F_A is due to buoyancy (Archimede's force), F_F to viscous friction and F_g to gravity.

where $U_h(s)$ is defined as

$$U_h(s) = C_h(s)P_h(s)R_C(s)\left[Y_d(s) - Y(s)\right] \tag{9}$$

being $Y_d(s)$ is the Laplace's transform of the reference signal. The term $U_C(s)$ is finally

$$U_C(s) = \left(\sum_{h=1}^{m} C_h(s)P_h(s)\right) R_C(s)\left[Y_d(s) - Y(s)\right] \tag{10}$$

that can be equated to its definition

$$U_C(s) = R_C(s)\left[Y_d(s) - Y(s)\right] \tag{11}$$

implying for the weights $P_h(s)$ that they must satisfy the (actuation) complementary condition

$$\sum_{h=1}^{m} C_h(s)P_h(s) = 1. \tag{12}$$

Overall, the closed loop system results in

$$Y(s) = G(s)\left(\sum_{h=1}^{m} C_h(s)P_h(s)\right) R_C(s)\left[Y_d(s) - Y(s)\right]. \tag{13}$$

3. AUV HEAVE MODEL

The proposed control solution is designed for the slender body AUV (Fig. 3) called Folaga described in [Caffaz et al., 2010]. The dynamic equations of this vehicle can be written as follows:

$$(M_I + M_A + m(t))\ddot{z}(t) = -\beta\dot{z}(t) + (M_I + m(t))g - \nabla\rho g + u_2(t) \tag{14}$$

and

$$\dot{m}(t) = -k\, m(t) + u_1(t) \tag{15}$$

where

M_I	Inertial mass of the vehicle.
M_A	Added mass.
$m(t)$	Mass of the fluid in the ballast tank at time t.
z	Depth of the vehicle.
β	Viscous friction coefficient in direction of z.
g	Gravity acceleration.
∇	Displacement.
ρ	Fluid density.
k	Inverse of the time constant of the ballast tank.
$u_1(t)$	Ballast tank control input.
$u_2(t)$	Heave control force generated by the electrical motors.

Equation (14) is relative to Newton's law along the heave axis [Fossen, 1994] while equation (15) models the dynamics of the fluid in the ballast tank. Notice that equation (15) is indeed an approximation of the ballast tank fluid dynamics: the in- and out- flows from the tank will actually have different time constants as the inflow is governed by a simple valve (the water entering the tank due to the higher pressure of environmental water) while the outflow is generated by an active pump. Moreover, both the input and output flows of the ballast tank fluid will depend on the depth of the vehicle. Yet for control design purposes, the ballast fluid mass is modeled with the simple linear first order equation in (15) that neglects these details.

Equations (14 - 15) imply

$$[M_A + M_I + m(t)]\dddot{z}(t) + \ddot{z}(t)[u_1(t) - km(t) + \beta] = \\ = [u_1(t) - km(t)]g + \dot{u}_2(t)$$

that is highly nonlinear due to the terms $m(t)$ and $u_1(t)$ multiplying the derivatives of $z(t)$: yet notice that $M_I + M_A \in [50, 100]$Kg while $m(t) \in [0, 0.35]$Kg, namely $m(t) \ll (M_I + M_A)$ implying that (14) can be approximated by the linear dynamics:

$$(M_I + M_A)\ddot{z}(t) = -\beta\dot{z}(t) + (M_I + m(t))g - \nabla\rho g + u_2(t) \tag{16}$$

Equations (15) and (16) allow to derive the transfer function model

$$\tilde{M} := M_A + M_I \tag{17}$$

$$\delta := (M_I - \nabla\rho)g \tag{18}$$

$$Z(s) = \frac{1}{s(\tilde{M}s + \beta)}\left(\frac{g}{(s+k)}U_1(s) + U_2(s)\right) + \\ + \frac{\delta}{s^2(\tilde{M}s + \beta)} \tag{19}$$

that corresponds to the structure in equations (7 - 8) noticing that

$$G(s) = \frac{1}{s(\tilde{M}s + \beta)} \tag{20}$$

and

$$U_C(s) = \frac{g}{(s+k)}U_1(s) + U_2(s) = \\ = C_1(s)\,U_1(s) + C_2(s)\,U_2(s) \tag{21}$$

being

$$C_1(s) = \frac{g}{(s+k)}, \quad C_2(s) = 1. \tag{22}$$

The last term on the right-hand side of equation (19) can be interpreted as a constant disturbance (matched with $U_C(s)$) that is null in case of perfectly neutral calibration, i.e. $M_I = \nabla\rho$.

4. CONTROL DESIGN

4.1 Controller

With reference to the model in equations (19 - 22), a possible simple controller able to reject the matched disturbance δ in equation (18) is a proportional - integral (PI) controller:

$$R_{PI} = K_{PI}\frac{\tau_{pi}s + 1}{s} \tag{23}$$

to be eventually implemented through an anti wind-up architecture [Åström and Hägglund, 1995]. As for the design of the spectral weight functions $P_1(s)$ and $P_2(s)$, given that the thrusters should be preferably used for the high frequency command components only, the corresponding spectral weight $P_2(s)$ is chosen to be a second order high-pass filter:

$$P_2(s) = \left(\frac{\tau_f s}{1 + \tau_f s}\right)^2. \tag{24}$$

Having defined $P_2(s)$ the spectral weight $P_1(s)$ for the ballast tank command follows directly from the complementary condition (12) resulting in:

$$P_1(s) = \frac{(2\tau_f s + 1)(s + k)}{g(1 + \tau_f s)^2}. \tag{25}$$

The parameter τ_f plays a fundamental role as it determines the threshold frequency identifying the low frequency region for the ballast tank control system as opposed to the high frequency region for the electric thrusters. Notice that this is exactly the counterpart of the situation in complementary filtering and, to some extent, in Kalman filtering. Indeed, the Kalman filter can be interpreted as a special complementary filter [Higgins, 1975] where the lower frequency measurement information is combined with the higher frequency model dynamics information to generate the Kalman state estimate.

The Bode plots of $C_1(s)P_1(s)$ and $C_2(s)P_2(s)$ are reported in figure 4 showing the complementary behavior of the thruster and ballast tank commands.

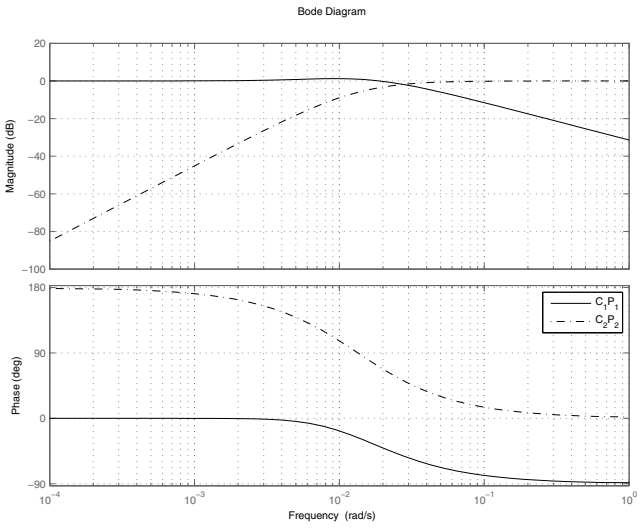

Fig. 4. Bode plots of $C_1(s)P_1(s)$, Low-Pass filter, and $C_2(s)P_2(s)$, High-Pass filter

$C_1(s)$		
g	9.81	$[m/s^2]$
k	8e-3	$[1/s]$

$P_2(s)$		
τ_f	80.8725	$[s]$

$P_1(s)$		
τ_f	80.8725	$[s]$
k	8e-3	$[1/s]$
g	9.81	$[m/s^2]$

$R_{PI}(s)$		
K_{PI}	0.1201	$[1/s]$
τ_{PI}	30	$[s]$

Table 1. Transfer function parameters used in the simulations.

4.2 Implementation issues

The proposed solution has been coded for experimental validation and simulation analysis. The presence of the integral action in (23) is necessary to reject the action of the matched disturbance δ defined in (18): yet given the limited capacity of the ballast tank and the relatively low power of the vertical thrusters, the integral action in the PI controller is likely to trigger actuation saturations. In order to cope with this, an anti wind-up implementation of the PI controller has been realized [Åström and Hägglund, 1995]. In particular, the block diagram of the (discretized) implementation is depicted in figure

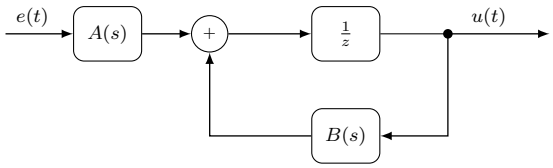

Fig. 5. The schema of Ant-WindUp implementation used in this work.

where $A(s)$ and $B(s)$ are defined as

$$A(s) = K\frac{\tau_{PI}s+1}{s+0.3}\,;\quad B(s) = \frac{0.3}{s+0.3} \tag{26}$$

5. SIMULATION RESULTS

The model in equations (14 - 15) used for control design does not explicitly account for the thruster and ballast tank actuation dynamics. In order to correctly simulate the control software to be eventually deployed on the Folaga AUV, the interface between the control signals $u_1(t), u_2(t)$ and the command signals of the Folaga robot has been developed and included in the simulations. In particular, the vertical thruster command of the Folaga vehicle is a signal in the range -100 and 100 with step of 10 corresponding to the motor PWM input. The ballast tank actuation is a valve for inflow and a motor pump for outflow. The physical command to the Folaga ballast tank actuation system may take only the values {-1, 0, 1} for the ejection, stop, and injection phases respectively. The actuator models used in the simulations are the following:

$$u_1 = \alpha_1\,\bar{u}_1,\quad \bar{u}_1 \in \{-1,0,1\} \tag{27}$$

$$u_2 = \alpha_2\,\bar{u}_2,\quad \bar{u}_2 = 10k\quad :\quad k \in [-10,10]\cap\mathbb{Z} \tag{28}$$

with

$$\alpha_1 = \text{1e-4 [Kg/s]} \tag{29}$$

$$\alpha_2 = 0.343\ \text{[N]}. \tag{30}$$

Although the actuator models in equation (27 - 28) are simplified versions of the physical actuator models, they still capture the low frequency behavior of the actuators as well as the structure of the command signals. The desired control signals $u_1(t)$ and $u_2(t)$ resulting from the designed control system (as in Fig. 2) and computed at each (discretized) time instant are used to determine the actuator commands $\bar{u}_1^*$ and $\bar{u}_2^*$ according to

$$\bar{u}_1^*(t) = \underset{\bar{u}_1\in\{-1,0,1\}}{\arg\min}\ |u_1(t) - \alpha_1\,\bar{u}_1| \tag{31}$$

$$\bar{u}_2^*(t) = 10\ \underset{k\in[-10,10]\cap\mathbb{Z}}{\arg\min}\ |u_2(t) - \alpha_2\,10k|\,. \tag{32}$$

The overall heave control system described has been test in simulation using a depth profile having the same geometry of the one described in [Caccia et al., 2003]. In particular, the AUV's surge velocity is assumed to be constant and equal to 0.1[m/s]. The reference heave profile is defined as follows:

$$z_d(t) = \begin{cases} 5 & \text{if } t \in [0;100]s \\ 5 - 0.04(t-100) & \text{if } t \in]100;200[s \\ 1 & \text{if } t \in [200;300]s \end{cases}$$

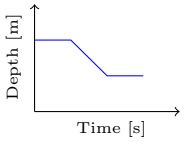

In order to illustrate the behavior of the proposed complementary actuation solution three types of simulations are performed: in the first two the vehicle is assumed to be initially neutral (i.e. $M_I = \nabla\rho$) and the proposed complementary solution is compared to the use of the thrusters only for the task of following the above $z_d(t)$ depth profile. A third simulation refers to a dive maneuver using the proposed complementary controller without being the vehicle neutrally buoyant. The simulation

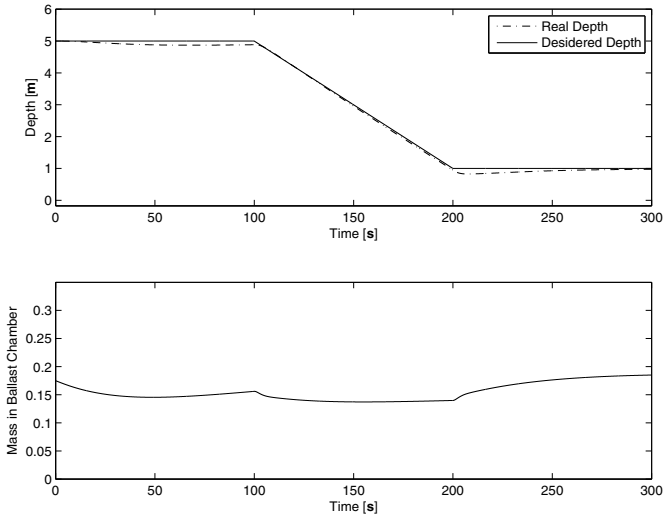

Fig. 6. Vehicle depth (top) and mass (bottom) of the water in the ballast chamber, using the proposed complementary solution.

results are illustrated in figures 6 to 10. In both cases

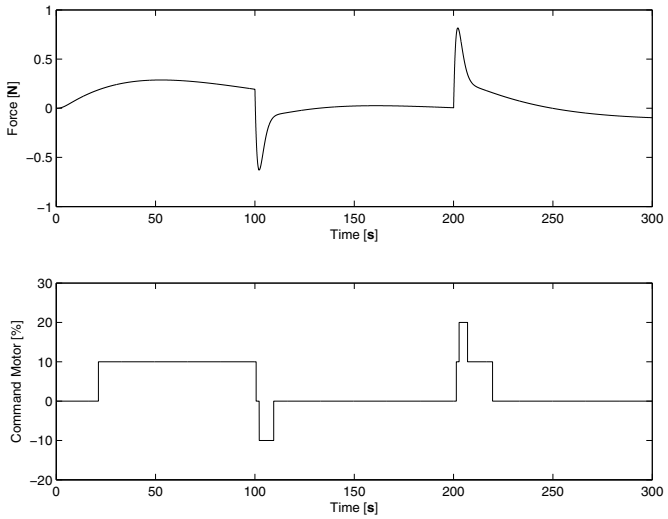

Fig. 7. Control effort of the thrusters for the simulation in figure 6.

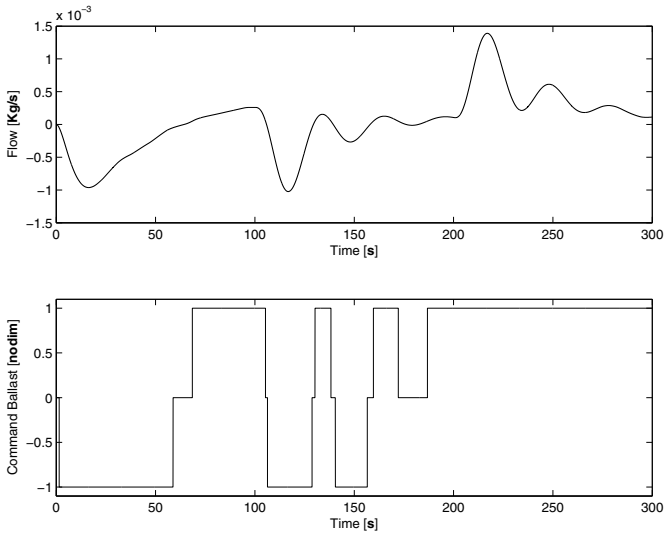

Fig. 8. Control effort of the ballast chamber actuator for the simulation in figure 6.

the control objective is achieved, but the time evolution of the thruster commands is obviously different. Notice, in particular, the difference in thruster usage during the "ramp" part of the depth profile in the two cases (figures 7 and 10). The results of the third simulation are shown in figures 11, 12 and 13: notice that as a result of stabilizing depth to a constant value through the proposed complementary controller (having a pole in the origin on the ballast chamber actuation channel only) the vehicle is automatically made neutrally buoyant. The depth is stabilized and the thrusters and ballast chamber actuator efforts converge to zero. The asymptotic value of the mass in the ballast chamber compensates the vehicle's mass, namely $\lim_{t\to\infty} \nabla\rho = M_I$. Indeed the proposed solution can be exploited to automatically calibrate the vehicle in order to make it neutrally buoyant.

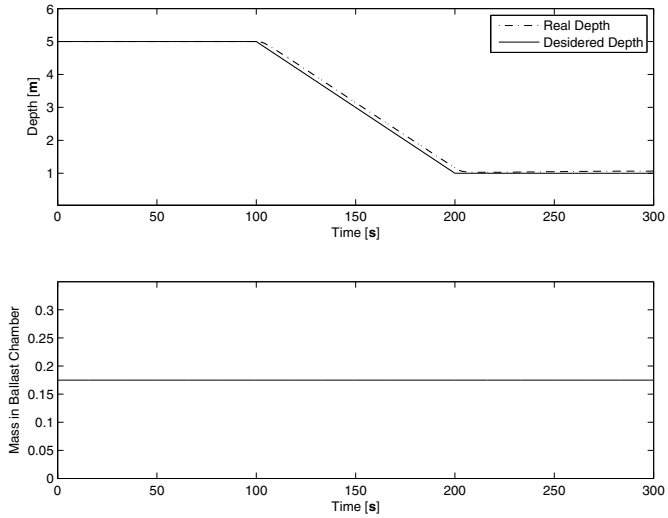

Fig. 9. Vehicle depth (top) and mass (bottom) of the water in the ballast tank, using the thrusters only.

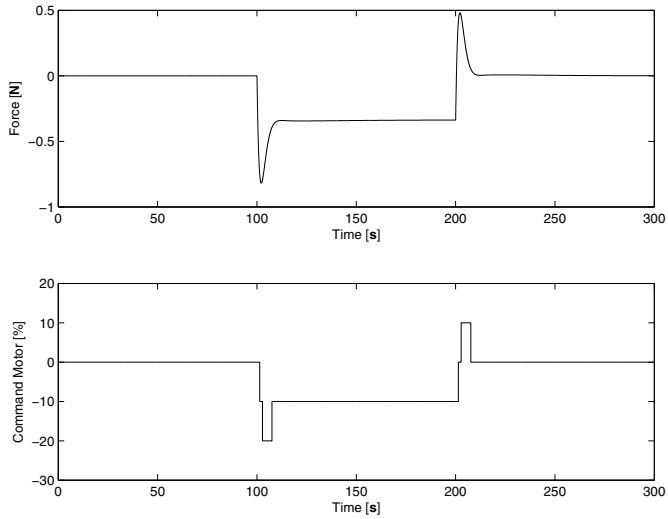

Fig. 10. Thrusters control effort for the case depicted in figure 9.

6. CONCLUSION

The depth control of an AUV having two actuator systems for the heave degree of freedom has been addressed: the two actuation systems are a i) ballast tank that can be filled or emptied changing the restoring force acting on the vehicle and ii) a set of vertical jet thrusters generating a vertical force. These two actuation systems have different dynamic behaviors: while the ballast tank system is relatively slow, the vertical jet thrusters have a much faster response. Inspired by the well know complementary filtering technique used in state estimation, the paper describes a "complementary actuation" controller design approach. A single PI controller (implemented through an anti wind-up architecture) is designed for the necessary vertical force to be generated in order to follow a depth profile. Such desired vertical force is decomposed in two signals corresponding to a lower frequency term and a (complementary) higher frequency one. The former is then generated through the ballast tank actuation system while the latter

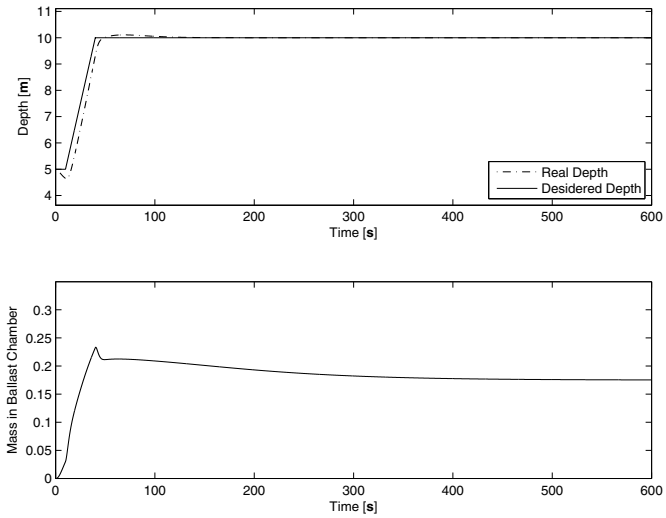

Fig. 11. Vehicle depth (top) and mass (bottom) of the water in the ballast chamber using the proposed complementary solution on a vehicle that is not initially neutrally buoyant.

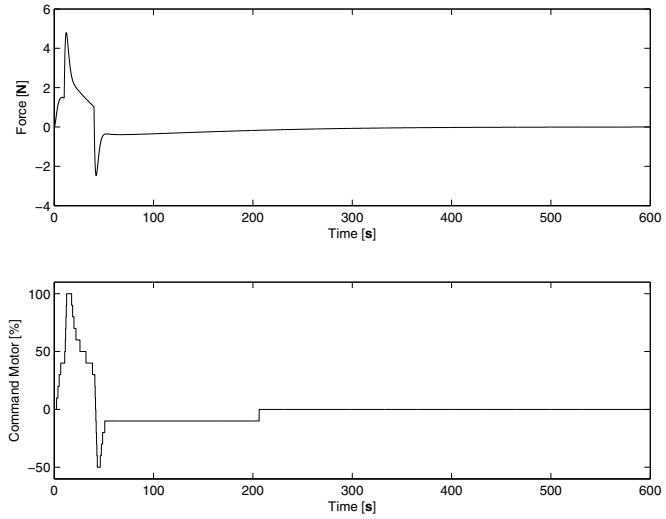

Fig. 12. Control effort of the thrusters for the motion profile depicted in figure 11.

is generated by the electrically powered vertical thrusters. As a result, the desired vertical force is seemingly generated by the concurrent operation of both actuation system each working in its most natural frequency spectrum. This is opposed to the factory built controller that uses either the ballast tank or the vertical thrusters to control the heave axis according to the mission specifications. The proposed solution is very simple in terms of realization and it has been proven to be effective in simulation. Given that the integral action of the designed PI controller is basically implemented by the ballast tank system, if the reference depth is constant the proposed solution leeds to an automatic neutrally buoyant calibration of the vehicle that, otherwise, needs to be obtained manually prior to starting the mission.

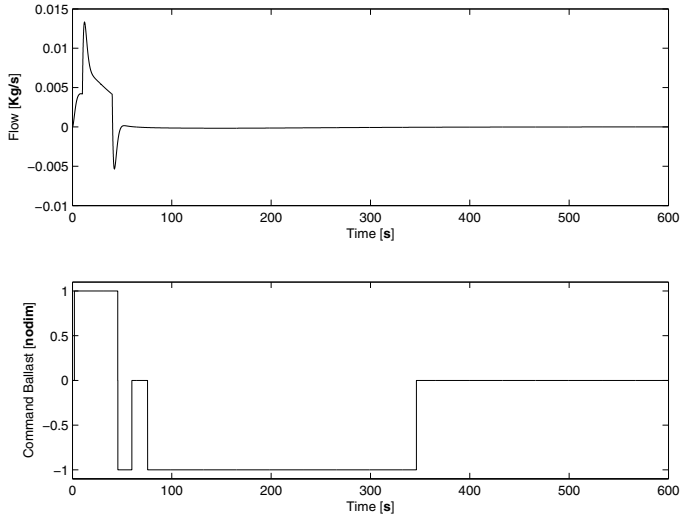

Fig. 13. Control effort of the ballast chamber actuator for the motion profile depicted in figure 11.

ACKNOWLEDGEMENTS

This work was partially supported by MIUR (Italian Ministry of Education, Universities and Research) under the PRIN project MARIS: Marine Autonomous Robotics for InterventionS, call of year 2010-2011, prot. 2010FBLHRJ.

REFERENCES

Alvarez, A., Caffaz, A., Caiti, A., Casalino, G., Gualdesi, L., Turetta, A., and Viviani, R. (2008). Folaga: A low-cost autonomous underwater vehicle combining glider and auv capabilities. *Ocean Engineering*, 36, 24–38. doi: 10.1016/j.oceaneng.2008.08.014.

Åström, K. and Hägglund, T. (1995). *PID Controllers: Theory, Design, and Tuning*. ISA: The Instrumentation, Systems, and Automation Society, 2 edition.

Caccia, M., Bono, R., Bruzzone, G., and Veruggio, G. (2003). Bottom-following for remotely operated vehicles. *Control Engineering Practice*, 11, 461–470. doi: 10.1016/S0967-0661(01)00142-3.

Caffaz, A., Caiti, A., Casalino, G., and Turetta, A. (2010). The hybrid glider/auv folaga. *Robotics & Automation Magazine, IEEE*, 17(1), 31–44. doi: 10.1109/MRA.2010.935791.

Cristi, R., Papoulias, F.A., and Healey, A.J. (1990). Adaptive sliding mode control of autonomous underwater vehicles in the dive plane. *Oceanic Engineering, IEEE Journal of*, 15(3), 152–160. doi:10.1109/48.107143.

Fossen, T.I. (1994). *Guidance and Control of Ocean Vehicles*. Wiley, 1 edition.

Higgins, W. (1975). A Comparison of Complementary and Kalman Filtering. *Aerospace and Electronic Systems, IEEE Transactions on*, AES-11(3), 321–325. doi: 10.1109/TAES.1975.308081.

Silvestre, C. and Pascoal, A. (2007). Depth control of the infante auv using gain-scheduled reduced order output feedback. *Control Engineering Practice*, 15(7), 883–895. doi:10.1016/j.conengprac.2006.05.005.

Zanoli, S. and Conte, G. (2003). Remotely operated vehicle depth control. *Control Engineering Practice*, 11, 453–459. doi:10.1016/S0967-0661(02)00013-8.